

# Strategy of bilayer structure of cellulose-based membrane with an efficient anti-fouling for solar-driven seawater desalination

Yuxuan Li · Jun Song\* · Jicheng Shan · Xiaosheng Qian ·

School of Material Science and Engineering, Tiangong University, Tianjin 300387,

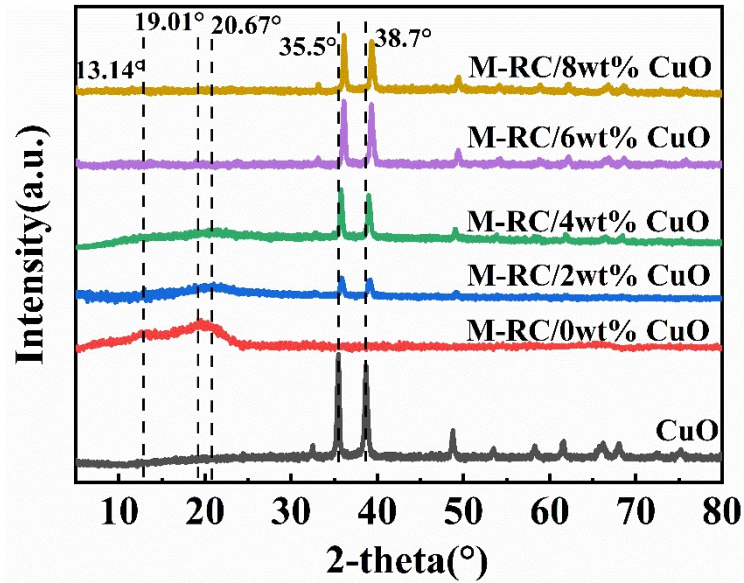
China

## Note S1

### Preparation of Hydrophilic RC/CuO Membrane (M-RC/CuO)

The pulp cellulose was initially dispersed in a three-necked flask containing DMAC (N,N-dimethylacetamide). The mixture was continuously stirred for 2 hours at 130°C under oil bath heating to facilitate the complete swelling of the cellulose. Subsequently, LiCl was added to the solution, and the temperature was reduced to 80°C, where stirring continued for 1 hour. After heating was ceased, stirring was maintained for an additional 18 hours, resulting in a homogeneous 6 wt% cellulose/ LiCl/DMAC solution. Copper oxide (CuO) with varying mass fractions (0, 2, 4, 6, and 8 wt%) was then added to the solution, followed by mechanical stirring to ensure uniform dispersion. The resulting CuO/cellulose/LiCl/DMAC composite solutions were labeled as follows: M-RC/0 wt%CuO (pure cellulose control), M-RC/2 wt%CuO, M-RC/4 wt%CuO, M-RC/6 wt%CuO, and M-RC/8 wt%CuO. This preparation process guarantees the uniform distribution of CuO particles within the cellulose matrix, providing a stable material system for further experiments.

## Note S2



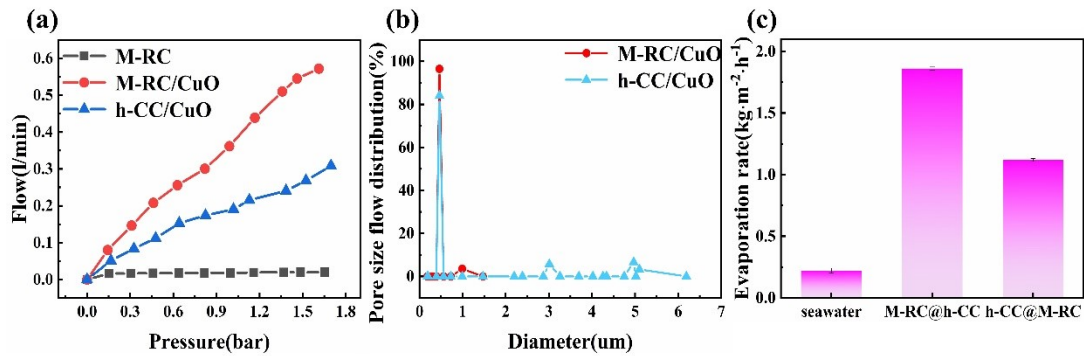
21

22 **Figure S1** (a) XRD pattern of M-RC/CuO membranes with different mass fractions

**Table S1** Lattice constants of M-RC membranes with different CuO mass fractions.

	CuO	M-RC /2wt%CuO	M-RC /4wt%CuO	M-RC /6wt%CuO	M-RC /8wt%CuO
a	4.68	8.01	8.04	8.07	8.01
c	5.13	4.53	4.45	4.48	4.47

23



24

25 **Figure S2** (a) Flow diagram of M-RC, M-RC/CuO, and h-CC/CuO;(b) Pore size

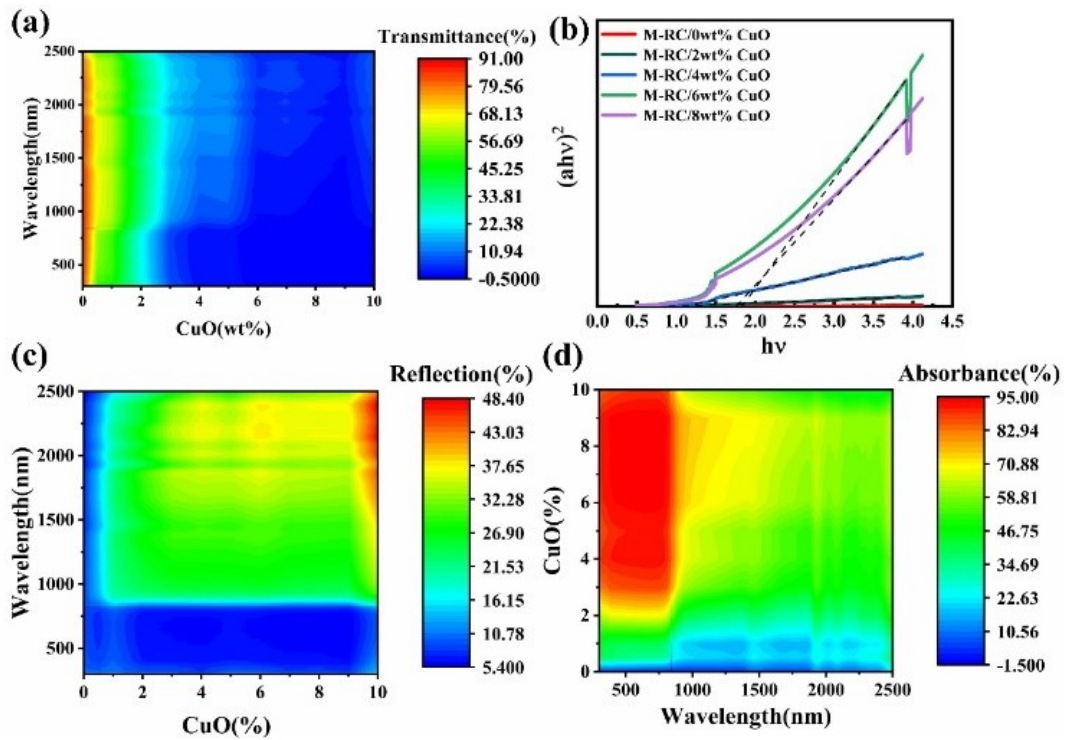
26 distribution diagram of M-RC/CuO and h-CC/CuO;(c) The evaporation rates of the

27 seawater, M-RC/CuO and h-CC/CuO membranes.

**Table S2** Optical band gaps of M-RC membranes with different CuO mass fractions.

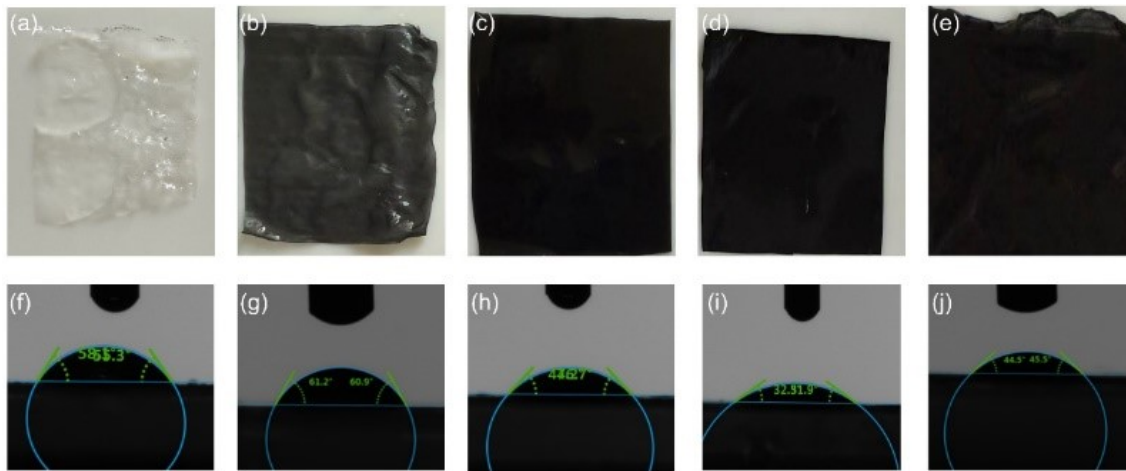
	M-RC/ 0wt%CuO	M-RC/ 2wt%CuO	M-RC/ 4wt%CuO	M-RC/ 6wt%CuO	M-RC/ 8wt%CuO
$E_g$ /eV	-	0.69	0.88	1.84	1.74

28



29

30 **Figure S3** Optical properties of M-RC/CuO membranes with different CuO mass  
 31 fractions: (a) transmittance; (b) optical band gap; (c) reflectance; (d) absorbance.



32

33 **Figure S4** (a)-(e) Surface morphology of M-RC/CuO membranes with different CuO  
 34 mass fractions; (f)-(j) Water contact angles of M-RC/CuO membranes with different  
 35 CuO mass fractions.

36 The surface emissivity ( $\epsilon = 0.38$ ) was determined based on experimental  
 37 reflectance measurements and calculated using a literature-reported method, expressed  
 38 as:

$$\varepsilon = \frac{\int_{0.3\mu m}^{2.5\mu m} [1 - R(\lambda)] P_{Sun}(\lambda) d\lambda}{\int_{0.3\mu m}^{2.5\mu m} P_{Sun}(\lambda) d\lambda} \# (1)$$

39

40 where  $R(\lambda)$  is the measured spectral reflectance and  $PSun(\lambda)$  is the normal solar  
 41 spectral irradiance defined by the ISO standard 9845-1 (1992) for air mass (AM) 1.5.

42 Figure S5 illustrates the experimental setup used to measure the convective heat  
 43 transfer coefficient. The setup primarily consists of a xenon lamp, the membrane  
 44 surface under test, and a temperature sensor system. The xenon lamp serves as a stable  
 45 heat source, irradiating the membrane surface, while fluid flows along the surface.  
 46 Temperature sensors are strategically placed on the membrane surface and in the  
 47 surrounding air to monitor both surface and fluid temperatures in real time, providing  
 48 essential data for the calculation of the convective heat transfer coefficient.

49 The convective heat transfer coefficient was determined using Figure S5, and the  
 50 following calculations were performed.

51 Calculation of the convective heat transfer coefficient

52 For natural convection on a horizontal surface, the relationship between the  
 53 Nusselt number (Nu) and the Rayleigh number (Ra) is shown in equation (2):

$$Nu = C \cdot Ra^n \# (2)$$

54

55 Where Nu is the Nusselt number, representing the ratio of convective heat transfer  
 56 to conductive heat transfer. Ra is the Rayleigh number, representing the ratio of  
 57 buoyancy-driven convection to viscous forces. C and n are constants that depend on the  
 58 specific geometry and flow conditions. For a vertical plane,  $C=0.59$ ,  $n=1/4$ .

59 The Rayleigh number is expressed as the product of the Grashof number (Gr) and  
 60 the Prandtl number (Pr), as shown in equation (3):

$$Ra = Gr \cdot Pr \# (3)$$

61

62 The Grashof number Gr represents the ratio of buoyancy-driven convection to  
 63 viscous forces, as shown in equation (4):

$$Gr = \frac{g \cdot \beta \cdot (T_S - T_\infty) \cdot L^3}{\nu^2} \#(4)$$

64

65 Where g is the acceleration due to gravity (9.81 m/s<sup>2</sup>),  $\beta$  is the coefficient of

66 volumetric expansion of air ( $1/300 \text{ K}^{-1}$ ),  $T_s$  is the temperature of the heated surface (41.2  
67 K),  $T_\infty$  is the ambient temperature (33.7 K),  $L$  is the characteristic length (0.04 m),  $\nu$  is  
68 the kinematic viscosity of air ( $1.51 \times 10^{-5} \text{ m}^2/\text{s}$ ).

69 The Prandtl number (Pr) is the ratio of momentum diffusion to heat diffusion, as  
70 shown in equation (5):

$$Pr = \frac{\mu \cdot C_p}{k} \#(5)$$

72 Where  $\mu$  is the dynamic viscosity of air ( $1.81 \times 10^{-5} \text{ kg/m}\cdot\text{s}$ ),  $C_p$  is the specific heat  
73 capacity of air ( $1005 \text{ J/kg}\cdot\text{K}$ ),  $k$  is the thermal conductivity of air ( $0.026 \text{ W/m}\cdot\text{K}$ ).

74 Finally, the heat transfer coefficient  $h$  is given by equation (6):

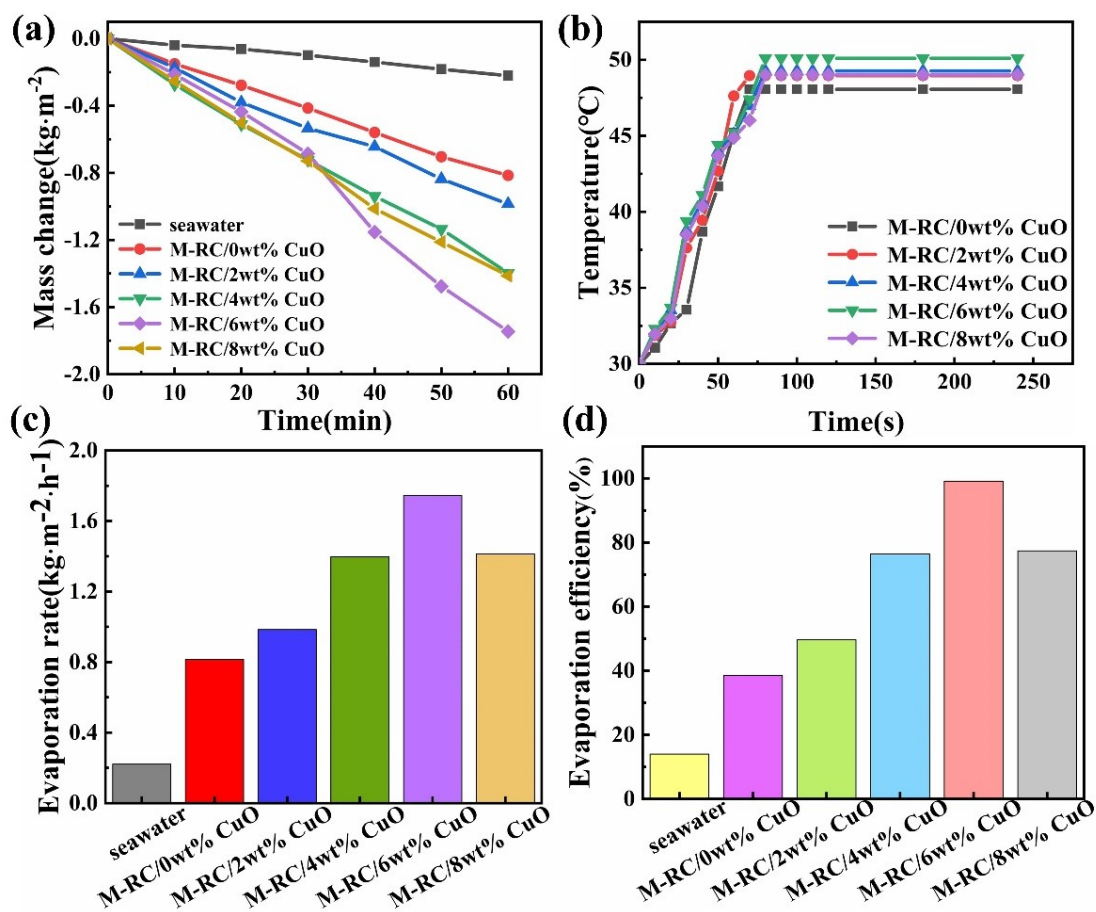
$$h = \frac{Nu \cdot k}{L} \#(6)$$

76 By performing the calculation,  $h$  is found to be  $1.60 \text{ W/m}^2\cdot\text{K}$ .



77

78 **Figure S5** Diagram of the device for measuring heat convection coefficient



79

80 **Figure S6** (a) Mass change; (b) surface temperature variation; (c) evaporation rate; and  
 81 (d) evaporation efficiency of M-Rc/CuO membranes with different CuO mass fractions  
 82 under one sun irradiation.